ACS Sustainable Chemistry & Engineering

Research Article

pubs.acs.org/journal/ascecg

Beyond Biodegradability of Poly(lactic acid): Physical and Chemical Stability in Humid Environments

Jeancarlo R. Rocca-Smith,[†,‡] Orla Whyte,[†] Claire-Helene Brachais,[§] Dominique Champion,[‡] Francesca Piasente,[∥] Eva Marcuzzo,[‡] Alessandro Sensidoni,[‡] Frederic Debeaufort,[†,⊥] and Thomas Karbowiak*[,†]

[†]Agrosup Dijon, UMR PAM A 02.102, Univ. Bourgogne Franche-Comté, Esplanade Erasme, 21000 Dijon, France

[‡]Department of Food Science, University of Udine, Via Sondrio 2/A, 33100 Udine, Italy

[§]ICMUB UMR-CNRS 5260 EMMD, Univ. Bourgogne Franche-Comté, 9 Allée Alain Savary, 21000 Dijon, France

[∥]Taghleef Industries, Via E. Fermi 46, 33058 San Giorgio di Nogaro (UD), Italy

[⊥]IUT Dijon-Auxerre, Department of BioEngineering, Univ. Bourgogne Franche-Comté, 7 Blvd Dr Petitjean, 21078 Dijon Cedex, France

ABSTRACT: Poly(lactic acid) (PLA) is the most traded biodegradable and biobased material. It is largely used as eco-friendly substitute of conventional plastics. Nevertheless, one of the main limiting factors is its water sensitivity. PLA reacts with water and is hydrolyzed during time, which determines its performance. Limited information related to the hydrolysis mechanism driven by water in vapor state is available in scientific literature. Literature is mainly focused on the effects of water in liquid state. This lack of information is of significant importance, since PLA interacts with water in both phases. This work was aimed to give a full depiction of the chemical and physical changes of PLA in a large range of relative humidity environments (from 50 to 100% RH) and in contact with liquid water. This research clearly showed that the stability of PLA was influenced not only by the chemical potential of water molecules, but also by their physical state due to a different behavior of degradation products. From a practical point of view, the findings of this study can be used as strong scientific basis for giving recommendations about the use of this material in its applications as packaging or mulch films.

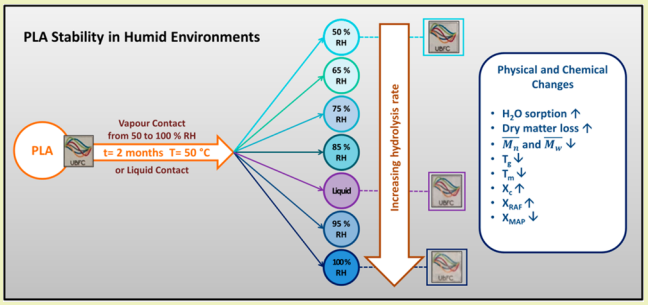

KEYWORDS: *Bioplastic, Aging, Hydrolysis, Amorphous phase, State of water*

INTRODUCTION

It is an undeniable fact that plastics have transformed our society since the beginning of their industrial production in the late 1940s.[1] Plastics materials are now ubiquitous and are used in almost all aspects of our daily life, such as in clothes, furniture, transport, buildings, electronic devices, and packaging.[1,2] They make our life more comfortable and also bring economic benefits to our society. Nevertheless, it is also unquestionable that conventional plastic waste materials (i.e., oil-derived and non-biodegradable) pollute and negatively affect our natural environment. Plastic wastes also contribute to the global warming, and they can last for a long time (several hundred years) as a waste in landfills. In addition, plastic wastes are vectors of harmful chemicals. They can transport and release toxic molecules to the environment such as bisphenols or phthalates, increasing the risk as well for the environment as well as human health.[1,3]

Bioplastics can be defined as plastics which are derived from natural resources, or are biodegradable, or have both properties.[4,5] They can substitute (partially or completely) conventional plastics in packaging applications and contribute to reduce the negative effects of conventional plastics.[6] Of the three most representative bioplastics on the market—30% biobased poly(ethylene terephtalate) (Bio-PET30), poly(lactic acid) (PLA), and biobased polyethylene (Bio-PE)—only PLA meets both the criteria of biosourcing and biodegradability.[4]

PLA derives from natural carbohydrate sources such as corn starch, sugar cane, wheat straw, and wood chips.[7] The production of PLA goods (e.g., films, rigid containers, bottles, and others) involves several steps that could be summarized as lactic acid production, polymerization, and industrial processing like extrusion, injection molding, blow molding, cast film extrusion, and thermoforming.[7−9]

PLA has largely been studied over the past two decades not only because of its eco-friendly nature, but also because of its high versatility. Compared to other biopolymers, PLA benefits of an interesting balance between cost, functional properties, and processability. Different strategies aiming at modifying

Received: December 18, 2016
Revised: January 26, 2017
Published: February 5, 2017

DOI: 10.1021/acssuschemeng.6b03088
ACS Sustainable Chem. Eng. 2017, 5, 2751−2762

bulk[10−14] and surface[15−18] properties of PLA are studied and adopted by research and industry to increase the PLA applications, particularly for the food industry.[19,20] However, one of the main limitations related to PLA polymer, especially for durable goods applications, is its inherent water sensitivity and biodegradability. Although PLA absorbs small quantities of water molecules (<1.1 wt% at T = 25 °C and close to saturation),[8,21] it reacts with water molecules and is hydrolyzed during time, compromising the performance of the PLA material.

Hydrolysis reduces the molecular weight of PLA and is considered as the first step of biodegradation, since it generates the metabolites for microbial degradation.[22] The hydrolysis mechanism of PLA has been principally studied for biomedical applications, and most of the related studies have been carried out in specific liquid media, which simulate biological systems.[23−26] For example, Makino et al.[27] in 1985 reported activation energy values around 83.5 kJ·mol^{-1} in PLA capsules stored in physiological saline solutions at temperatures between 21 and 45 °C, which means that the reaction is around 3 times accelerated for 10 °C of temperature increase. Nevertheless, the main application of PLA is currently as industrial films, and according to their final use (e.g., packaging or mulch films), they can be exposed to numerous environments having various pH, relative humidity (RH), and temperature. In addition, the interactions with water are not only limited to the liquid state, but also occur in the vapor state. Although all these different conditions are known to influence chemical reactions, only scarce information related to their influence on the stability of PLA is reported in literature.

Based on these considerations, the objective of the present work was to study the modifications induced on PLA films when they are exposed to water environments in the vapor or in the liquid state. To that aim, an accelerated aging study was carried out under seven wet condition environments to cover a wide range of situations. The PLA films were placed at 50, 65, 75, 85, 95, and 100% RH or immersed in liquid water at 50 °C. Macroscopic, chemical, and physical modifications were assessed over a long time period of 70 days.

EXPERIMENTAL SECTION

PLA Films. Semicrystalline PLA films (D-level ≥ 4.25%), industrially processed and commercially available for food packaging applications, were used in this study (Nativia NTSS, Taghleef Industries, Udine, Italy). During industrial processing, PLA films were subjected to biaxial stretching and annealing to induce crystallization and to improve their mechanical properties. The technical characteristics of the films used are thickness = 20 μm, water vapor transmission rate = 440 g·m^{-2}·d^{-1} (38 °C, 90% RH), and oxygen transmission rate = 1100 cm^3·m^{-2}·d^{-1} (23 °C, 0% RH). The thickness of films was measured in at least five different positions using a micrometer (Coolant Proof micrometer IP 65, Mitutoyo, Aurora, IL, USA).

Sample Preparation and Controlled Storage Conditions. The commercial PLA films were first submitted to primary vacuum (EKF56CX-4, ABM Greiffenberfer, Marktredwitz, Germany) for 3 days at room temperature (23 ± 2 °C), to remove any water and volatile molecules entrapped in the polymer matrix. Rectangular samples of 20 cm^2 (5 × 4 cm) or 10 cm^2 (5 × 2 cm) were initially weighed. Samples mass was ∼50.0 mg (±0.2) or 25.0 mg (±0.5), respectively. PLA samples were then placed in 10 mL vials and stored in different microclimate chambers at 50 °C for 70 days. The storage temperature chosen was able to accelerate the chemical reactions, without inducing strong modifications in the physical state of PLA, such as transitions from glassy to rubbery state, since it was 5−10 °C lower than the glass transition temperature (T_g). Seven storage conditions were considered in this study. For studying the impact of the water molecules in the vapor state, 20 cm^2 surface area PLA samples were exposed to environments at ∼50, 65, 75, 85, 95, and 100% RH, using saturated salt solutions of NaBr (Sigma-Aldrich, St. Louis, MO, USA), KI (Sigma-Aldrich), NaCl (Sigma-Aldrich), KNO_3 (Riedel-de Haën, Morristown, NJ, USA), K_2SO_4 (Sigma-Aldrich), and distilled water, respectively.[28] Concerning the impact of water molecules in the liquid state, 10 cm^2 surface area PLA samples were immersed in 10 mL distilled water. Three to four samples were collected every week of each storage condition. These aged samples were then equilibrated at room temperature at least for 2 h. They were weighed before and after been dried up to equilibrium, under primary vacuum from 3 to 7 days at room temperature. In the case of immersed samples in liquid water, samples were removed from the liquid, rinsed with distilled water. The excess of water was removed using tissue paper before submission to primary vacuum in same conditions. The dried samples were then stored at −30 °C up to analyses.

Physical and Chemical Characterizations. *Water Content and Dry Matter Variation.* The water content and the dry matter variation of PLA samples were measured gravimetrically and calculated according to eqs 1 and 2, respectively.

$$\text{water content (\%)} = \frac{m_{wt} - m_{dt}}{m_{dt}} \times 100 \quad (1)$$

$$\text{dry matter variation (\%)} = \frac{m_{dt} - m_{di}}{m_{di}} \times 100 \quad (2)$$

where m_{wt} is the wet mass (g) of the sample at time t, m_{dt} is the dry mass (g) of the sample at time t, and m_{di} is the initial dry mass of the sample (g), before starting the storage test. The analyses were completed in triplicates.

pH. The pH of the liquid water in contact with the samples was analyzed during time using a pH meter (C561, Consort, Turnhout, Belgium) equipped with a pH electrode (VWR, Radnor, PA, USA). The calibration of the device was conducted using standard solutions at 4 and 7 pH (high-resolution pH buffer, Fischer Scientific, Pittsburgh, PA, USA). The initial pH of the liquid water was 5.7. Samples were equilibrated at room temperature before being analyzed. The analysis was done in triplicate.

Molecular Weight Distribution. The molecular weight distribution of the PLA samples was analyzed during time by size-exclusion chromatography (SEC), using a 1260 Infinity liquid chromatography system (Agilent Technologies, Santa Clara, CA, USA). The device was composed of two polypore size exclusion columns (Agilent Technologies) connected in series. PLA samples (∼50 or 25 mg) were completely dissolved in 1 mL of tetrahydrofuran (THF, Carlo Erba reagents, Val de Reuil, France) using a shaker (PL-SP 260VS, Agilent technologies) for 20 min at room temperature. The dissolved samples were then filtrated using a syringe filter with a poly(tetrafluoroethylene) (PTFE) membrane (pore diameter 0.2 μm, Dominique Dutscher SAS, Brumath, France) and transferred in 1.5 mL vials. A 10 μL sample was automatically injected in the instrument. Filtered THF with a constant flow rate of 1 mL·min^{-1} was used as the mobile phase, and a refractive index detector was used in this analysis. The separation was carried out at a controlled temperature of 45 °C. Polystyrene standards ranging from 1.28 to 1820 kDa (Advancing Polymer Solutions, Agilent Technologies) were used for calibration curve. The number-average molecular weight ($\overline{M}_n$), the weight-average molecular weight ($\overline{M}_w$), and the polydispersity index (PDI) were calculated from the experimental molecular weight distribution curve using Agilent GPC/SEC software (version 1.2, Agilent Technologies). The analysis was conducted in duplicates.

Thermal Transitions. The thermal transitions of PLA films were studied by differential scanning calorimetry (DSC) using a Q20 calorimeter (TA Instruments, New Castle, DE, USA). Samples were weighed (3−5 mg) and sealed into airtight aluminum pans (Tzero, T.A. Instruments) before being subjected to a double heating−cooling

DOI: 10.1021/acssuschemeng.6b03088
ACS Sustainable Chem. Eng. 2017, 5, 2751−2762

cycle at 10 °C·min^{-1} under N_2 atmosphere (flow rate of 25 mL·min^{-1}).

Two different heating programs were used. The first program consisted in a double heating cycle in a narrow temperature range (from −10 to 100 °C) to focus only on the thermal events related to the mobile amorphous phase of PLA. The first cycle of this heating program allowed us to remove the excess of enthalpy associated with the glass transition, while the second one allowed us to better estimate the variation of specific heat (ΔC_p) and the glass transition temperature (T_g inflection point). The second program was performed on a broader temperature range (double heating from −10 to 190 °C) to study the transitions related to the crystalline phase of PLA, such as melting temperature (T_m) and melting enthalpy (ΔH_m). In this case, the thermal parameters were estimated from the first heating, while the reversibility of the overall transitions was assessed from the second heating. At least two samples were run for each heating program, and the thermal parameters were determined using TA Universal Analysis 2000 software (version 4.5 A, TA Instruments).

The crystallinity percentage (X_c) was calculated according to eq 3.

$$X_c = \frac{\Delta H_m - \Delta H_{cc}}{\Delta H_m^0} \times 100 \quad (3)$$

where ΔH_m (J·g^{-1}) is the enthalpy corresponding to the area under the melting peak, ΔH_m^0 (= 93 J·g^{-1})[29] is the enthalpy of melting of pure crystalline PLA, and ΔH_{cc} (J·g^{-1}) is the enthalpy corresponding to the area associated with cold crystallization. Since no cold crystallization was observed in the first heating of the program related to the crystalline phase study, its value is null (ΔH_{cc} = 0 J·g^{-1}).

The percentage of mobile amorphous phase (X_{MAP}) and the percentage of the rigid amorphous fraction (X_{RAF}) in the PLA films were also calculated during time, according to Arnoult et al.,[30] (eqs 4 and 5, respectively).

$$X_{MAP} = \frac{\Delta C_p}{\Delta C_p^0} \times 100 \quad (4)$$

$$X_c + X_{MAP} + X_{RAF} = 100\% \quad (5)$$

where ΔC_p is the measured variation of specific heat for the glass transition associated with the mobile amorphous phase, and ΔC_p^0 is that corresponding to a 100% amorphous PLA sample (ΔC_p^0 = 0.48 J·g^{-1}·K^{-1}).[30,31] Since two glass transitions were observed in the mobile amorphous phase, during the second heating of the first DSC program, the ΔC_p used in the formula was the sum the both transitions ($\Delta C_p = \Delta C_{p1} + \Delta C_{p2}$).

Kinetics Analysis. The experimental values of crystallinity percentage (X_c), the number-average molecular weight ($\overline{M}_n$), and the weight-average molecular weight ($\overline{M}_w$) over time were modeled using a zero and first apparent order kinetics (eqs 6, 7, and 8).

$$X_c = X_{c0} \pm k_{app(X_c)} t \quad (6)$$

$$\ln \overline{M}_n = \ln \overline{M}_{n0} \pm k_{app(\overline{M}_n)} t \quad (7)$$

$$\ln \overline{M}_w = \ln \overline{M}_{w0} \pm k_{app(\overline{M}_w)} t \quad (8)$$

where X_{c0}, $\overline{M}_{n0}$, and $\overline{M}_{w0}$ are the crystallinity percentage, the number-average molecular weight, and the weight-average molecular weight of initial PLA, respectively. t is the time (day). $k_{app(X_c)}$, $k_{app(\overline{M}_n)}$, and $k_{app(\overline{M}_w)}$ are the corresponding apparent rate constants (in %·day^{-1}, day^{-1}, and day^{-1}, respectively). The corresponding apparent rate constants (k_{app}) were estimated using the statistic software GraphPad Prims 5 (version 5.04, GraphPad Software, Inc., La Jolla, CA, USA). Rate constants were considered significantly different when no intersection in their 95% confidence interval was found.

RESULTS AND DISCUSSION

Macroscopic Modifications of PLA Films during Aging. Some simple measurements such as water content, dry matter variation, and pH already provided a useful depiction of the stability of PLA submitted to accelerated aging.

Water Content. When PLA was stored in contact with water molecules from the vapor phase (50, 65, 75, 85, 95, and 100% RH), the PLA capacity to sorb water clearly increased with time and with RH (Figure 1a). Whatever RH, the water content

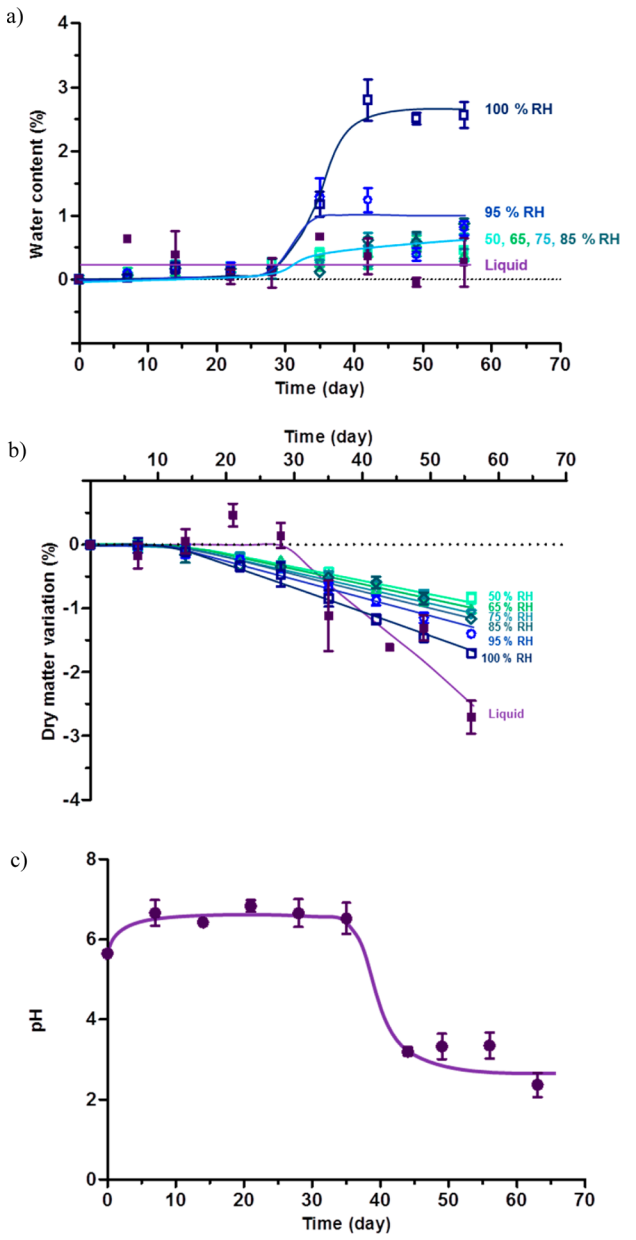

Figure 1. Water content (a), dry matter variation (b), and pH kinetics (c) of PLA films stored at 50, 65, 75, 85, 95, and 100% RH or immersed in liquid water at 50 °C. Error bars are standard deviations. Lines are guides for the eyes.

remained constant and close to 0% during the first month of storage. After that time, the water content increased and reached a pseudo-plateau of ∼1 and 2.5% for the samples stored at 95 and 100% RH, respectively. A similar but slighter behavior was also observed in the samples stored at the lower RH conditions (50, 65, 75, and 85% RH), which reached a lower water content value (∼0.5%) by the end of the test. Such increased capacity of PLA to sorb water molecules, after a

DOI: 10.1021/acssuschemeng.6b03088
ACS Sustainable Chem. Eng. 2017, 5, 2751−2762

relatively long induction time, can be considered in line with the effects of PLA hydrolysis. It is well known that even if PLA sorbs small quantities of water molecules (<1.1 wt% at T = 25 °C and close to saturation),[8,21] it can react and be hydrolyzed by them, generating degradation products.[23,24] The degradation products of PLA (e.g., lactic acid and its oligomers) have an increased density of polar groups (e.g., hydroxyl and carboxyl) compared to the initial polymer and are continuously produced over time. Therefore, an enhanced water affinity is expected to occur in the PLA samples under hydrolysis, as a consequence of the exposition of new water sorption sites. Several studies have also reported that hydrolysis of PLA, driven by water molecules from the vapor phase, induces a significant rise in the water sorption capacity.[32−34] As an example, Cairncross et al.[34] reported an increase of 2 and 10 times of the water quantity sorbed by PLA films after storage for 2 and 3 days, respectively, at 85% RH and 80 °C. Accordingly, we can suggest that the PLA samples from the present study were hydrolytically degraded, when they were stored in contact with water vapor molecules. This even started at 50% RH, and the degradation was probably faster in the samples stored at the highest RH, as suggested by the increase in water uptake.

When PLA was immersed in liquid water, a totally different behavior was observed (Figure 1a). The water content did not highly increase as in vapor contact, but oscillated around a rather low value (~0.25%) during the entire storage test. Lyu et al.[35] already reported a similar behavior in PLA discs stored in liquid media (pH 7.4) for ~400 days at 37 °C. They detected a very low and constant water content (~0.01 wt%), even if such samples were highly hydrolytically degraded over time, with tremendous decrease of the $\overline{M}_n$ value from 290 kDa to ~20 kDa. An increase in the water content was only observed when the PLA disks were degraded to lower $\overline{M}_n$ values. These results of Lyu et al.[35] suggested that a simple water content analysis cannot be only itself a good indicator of the hydrolysis reaction, especially when high-molecular-weight PLA is hydrolyzed in liquid media. In these conditions, a mass transfer of degradation products from the polymer into the liquid media is possible, due to their high polarity and small size. Such molecules, offering additional sorption sites for water, thus do not accumulate in the polymer matrix, as it occurs when the hydrolysis is driven by water molecules in vapor phase. Therefore, hydrolysis cannot be simply discarded on the basis of low water uptake for PLA samples immersed in liquid water.

Dry Matter Variation. Now considering the change in the dry matter, all PLA samples progressively lost dry mass after a lag time, whatever the state of water with which it is in contact (Figure 1b).

PLA samples immersed in liquid water were characterized by the longest lag time (~30 days) and the highest dry matter loss (~3% after ~2 months of storage). Similar decreasing trends were also observed in degradation studies of semicrystalline PLA films produced by annealing[26,36] or by stereocomplexation[37] and immersed in buffer solutions (pH 7.4) at 37 °C, as well as in degradation studies of PLA plates[38] and PLA discs[35] exposed to similar aqueous media. As an example, Tsuji and Ikada[26] reported an induction time of 12 months and a decrease in the dry mass of around 10 to 38% in semicrystalline PLA films (X_c > 40%) after 36 months storage in a phosphate buffer solution at 37 °C.

The decrease in the dry mass unambiguously confirmed the generation of compounds able to be solubilized and transferred to the liquid media, as previously hypothesized. The time needed to detect such decrease perfectly matched the time corresponding to a high increase of the water content in PLA samples stored in saturated vapor conditions (~30 days, Figure 1a). This strongly suggested that the hydrophilic compounds able to induce a higher sorption capacity in the samples exposed to 100% RH were, at the same time, highly water soluble, possibly because of their small size and high polarity.

Considering the PLA samples stored in contact with water vapor molecules (50, 65, 75, 85, 95, and 100% RH) the lag time was around 10 days. The loss of dry matter progressively increased at higher RH conditions (~0.8, 1.0, 1.1, 1.2, 1.4, and 1.7%, respectively). These results thus indicated an increasing capacity of PLA to release volatile molecules, when PLA was stored in environments at increasing RH. This phenomenon was unexpected, since degradation products such as lactic acid and its oligomers are low-volatility compounds. Only a few studies have reported a dry matter loss in PLA when it is stored in humid atmospheres,[33,39] and not enough explanation of such phenomenon has been provided, since a large quantity of hydrolytic degradation studies has been carried out in liquid environments. There are several reasons that could explain such behavior, like hydrolysis-induced release of impurities or solvent residuals entrapped in the polymer matrix, or most likely volatiles formation from oxidation reactions. In fact, it could be possible that molecular oxygen (O_2) reacts with compounds already included in the matrix (e.g., impurities, solvents residuals, additives, etc.) or continuously formed during hydrolysis, generating free radicals and volatiles (e.g., ketones, aldehydes, etc.). This hypothesis could explain the shorter induction time of the dry mater variation of these samples in contact with water vapor compared to the PLA immersed in liquid water. In that case, oxidation reactions should be limited by the presence of liquid water molecules, which surround the sample and act as a barrier to O_2. In contrast, when PLA is exposed to water molecules in the vapor state, it is also directly exposed to O_2, thus favoring oxidation reactions.

pH. The variation in the pH of the liquid water in contact with PLA was also followed during aging (Figure 1c). A significant increase from an initial value ~5.5 to ~6.5 was observed during the first week of aging. After that time, the pH remained constant until the fifth week of storage (~35 days) and then rapidly decreased to ~3.0.

The initial increase in pH was probably a consequence of alkaline compounds release, which may be incorporated during industrial production for enhancing the PLA performance. It is known that including alkaline compounds (e.g., magnesium oxide, tricalcium phosphate, caffeine, and coral) is a suitable strategy to limit the hydrolysis reaction in PLA. Such compounds are able to neutralize the carboxyl groups of the degradation products, which are at the same time catalysts of the reaction.[23,24] Then, the fast decrease of the pH indicated that soluble and acidic compounds were generated after 35 days, confirming therefore that the mass loss was due to a mass transfer into the liquid medium in the form of soluble and acidic degradation products.

Similar pH trends were also noticed in other hydrolytic studies done on PLA films immersed in liquid water at 58 °C,[22] and PLA-based composites immersed in buffer solutions (pH 7.4) at 60 °C,[40] as well as in PLA plates placed in buffer solutions at pH 7.4 and 3.7 at respectively 60 and 37 °C.[38]

DOI: 10.1021/acssuschemeng.6b03088
ACS Sustainable Chem. Eng. 2017, 5, 2751−2762

Modifications in the Molecular Weight Distribution Induced by Aging. In order to better understand the effects of the RH and the effect of the physical state of the water molecules on PLA films, the molecular weight distribution in average number ($\overline{M}_n$), the molecular weight distribution in average weight ($\overline{M}_w$), and the polydispersity index (PDI) of PLA samples stored in all the conditions were assessed over time (Figure 2).

As suggested by the macroscopic analyses, a significant decrease in $\overline{M}_n$ and $\overline{M}_w$ was observed in all of the conditions. Thereby, it confirmed that all PLA films were subjected to hydrolysis (Figure 2a,b). $\overline{M}_n$ decreased from an initial value of around 93 kDa to 66, 51, 40, 20, 5, 5, or 12 kDa after being stored at 50, 65, 75, 85, 95, or 100% RH or in liquid conditions, respectively, for 70 days at 50 °C. Similarly, the corresponding $\overline{M}_w$ values decreased from around 190 kDa to 140, 110, 86, 51, 10, 10, or 25 kDa. This decreasing trend for both parameters followed a first apparent order, in agreement with several degradation studies carried out in liquid water or in water vapor conditions.[22,38,39,41−44]

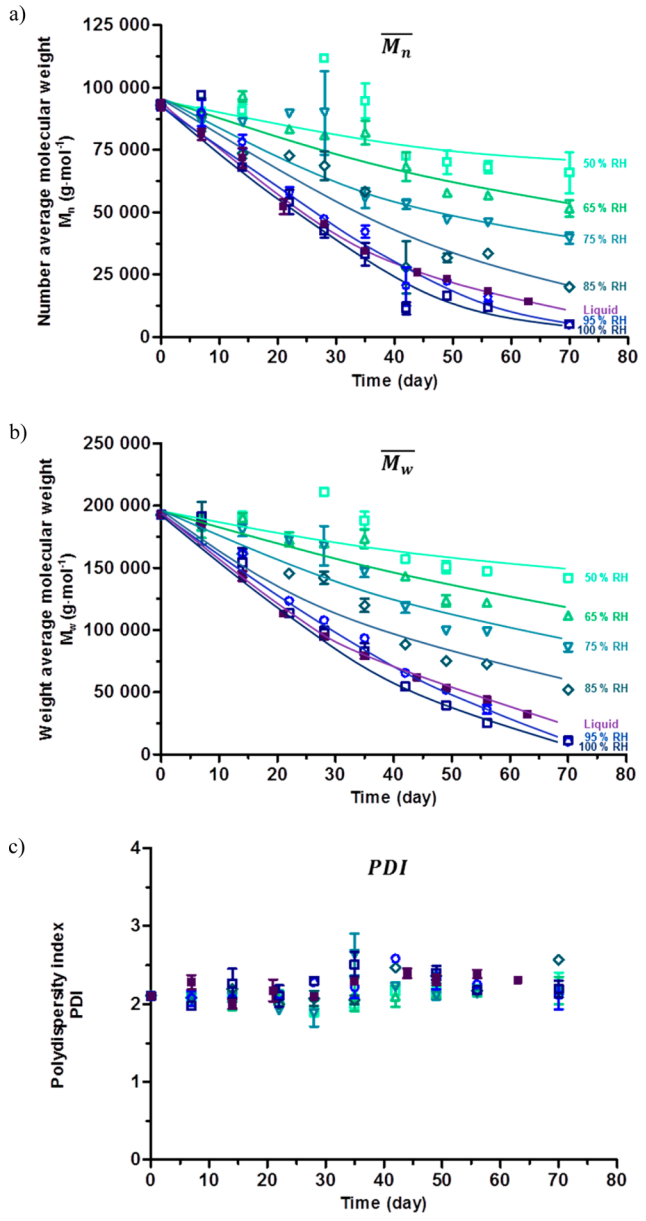

Figure 2. Kinetics of the molecular weight distribution of PLA films stored at 50, 65, 75, 85, 95, and 100% RH or immersed in liquid water at 50 °C: (a) number-average molecular weight ($\overline{M}_n$), (b) weight-average molecular weight ($\overline{M}_w$), and (c) polydispersity index (PDI). Error bars are standard deviations. Lines are guides for the eyes.

The kinetic analysis of $\overline{M}_n$ and $\overline{M}_w$ pointed out some differences in the hydrolysis mechanism of PLA, associated with the RH and physical state of water molecules (Table 1). On the one hand, when PLA was stored in wet atmospheres, a progressive and significant acceleration in the apparent reaction rate occurred when RH increased, with respect to the chemical potential of water. On the other hand, when PLA was immersed in liquid water, the apparent reaction rate was higher than conditions below 85% RH, but lower for 95 and 100% RH. In this case, the chemical potential of water molecules cannot fully account for the reaction rate. The chemical potential of the liquid water molecules can be considered equivalent to the chemical potential of the water vapor molecules in saturated conditions (100% RH). This means, from a theoretical point of view, that both environments should induce similar hydrolysis rates. Nevertheless, kinetics of $\overline{M}_n$ and $\overline{M}_w$ clearly indicated that the hydrolysis was significantly slower when PLA was immersed in liquid water.

Such deviation could result from the solubilization of the degradation products of small size, which act at the same time as catalysts of the reaction.[23,24] As evidenced by previous macroscopic analysis, these acidic molecules were transferred to the liquid media when PLA was immersed in liquid water, which therefore limit or annihilate their action as catalysts. On the contrary, when PLA was exposed to water vapor, the degradation products were accumulated in the polymer matrix, accelerating therefore the reaction. This hypothesis was further strengthened by the decrease in $\overline{M}_w$ and $\overline{M}_n$ for both conditions (Figure 2a,b). The deviation in this decreasing trend was evident after 40 days storage in liquid water. This time was close to the time from which the soluble acidic molecules released in the liquid media modified the pH (~30 days). The key role of the degradation products has also been reported in hydrolytic studies of PLA goods of big sizes (thickness between 0.5−2 and 7.4 mm) carried out in aqueous media.[23−25,33] Such hydrolytic conditions favor an accumulation of the degradation products in the core of the PLA material. In a similar way to the present study, it allows a faster degradation in the bulk than in the surface, where the degradation products can be easily dissolved in the liquid media.[23−25,33]

The hydrolysis did not highly influence the polydispersity index (PDI) (Figure 2c). The PDI oscillated around its initial value ~2.1, and no particular trend was observed at any storage condition. When the hydrolysis mechanism favors the formation of small or big oligomers in a preferential way, an increase or decrease of PDI is expected, respectively. These results thus suggested that the PLA chains were randomly hydrolyzed or end chain degraded in all the storage conditions. This behavior was also confirmed by the monomodal molecular weight distribution curve, which moved to low molecular weights when time increased, but without any change in the curve width, and no apparition of new peaks. Similar findings were also reported in others studies, involving the degradation of PLA films in aqueous media for one and two months at 37 and 58 °C, respectively,[22,45] as well as in degradation studies of

DOI: 10.1021/acssuschemeng.6b03088
ACS Sustainable Chem. Eng. 2017, 5, 2751−2762

Table 1. Kinetic Parameters of Number-Average Molecular Weight Loss ($\overline{M}_n$), Weight-Average Molecular Weight Loss ($\overline{M}_w$), and Crystallinity Percentage Increase (X_c) of PLA Films Stored in Different Wet Environments at 50 °C for 70 Days

		storage conditions						
	parameter[a]	50% RH	65% RH	75% RH	85% RH	95% RH	100% RH	liquid
$\overline{M}_n$	k_{app} ($day^{-1}\cdot10^{-3}$)	5.9^{a}	9.6^{a}	14.0^{ab}	23.0^{bc}	40.5^{de}	43.7^{e}	30.5^{cd}
	95% CI	1.3−10.6	7.0−12.2	9.5−18.5	16.3−29.7	31.4−49.5	35.1−52.3	28.7−32.3
	R^2	0.56	0.90	0.87	0.89	0.93	0.94	0.99
$\overline{M}_w$	k_{app} ($day^{-1}\cdot10^{-3}$)	5.1^{a}	8.6^{ab}	13.0^{b}	19.7^{c}	38.5^{de}	40.7^{e}	28.4^{d}
	95% CI	2.0−8.2	6.2−11.0	10.0−16.0	16.8−22.6	28.4−48.6	33.8−47.6	26.5−30.3
	R^2	0.68	0.90	0.93	0.97	0.91	0.96	0.99
X_c	k_{app} (%·$day^{-1}\cdot10^{-2}$)	2.3^{a}	3.6^{a}	8.9^{b}	14.9^{c}	18.8^{c}	19.8^{c}	17.9^{c}
	95% CI	0−5.7	1.6−5.6	7.2−10.6	13.4−16.4	13.5−24.1	14.8−24.9	15.0−20.7
	R^2	0.48	0.86	0.98	0.99	0.96	0.97	0.99

[a] k_{app} is the apparent rate constant (first apparent order for $\overline{M}_n$ and $\overline{M}_w$ and zero apparent order for X_c), 95% CI indicates the 95% confidence interval, and R^2 is the coefficient of determination. The rate constants were considered significantly different when no intersection was found in their 95% confidence interval. k_{app} values followed by the same superscript letter within a row are not significantly different at p-level 0.05; different letters in the same row mean significant difference.

PLA fibers exposed to environments at 100% RH, for 3 months at 40 °C.[39] The results of this study also agreed with the considerations made by Gleadall et al.[46] in a study involving data modeling of 31 scientific papers. These authors concluded that the hydrolysis of PLA is carried out by a combination of random and end chain scission mechanisms.[46] According to these authors, one mechanism cannot fully explain the behavior of PLA during degradation, since the random scission mechanism is behind the fast decrease in molecular weight of PLA, while the end chain scission mechanism is behind the mass reduction of the polymer, as it produces soluble monomers.[46]

Modifications in the Thermal Transitions Induced by Aging. The effect of hydrolysis in the physical structure of PLA was further investigated by differential scanning calorimetry (DSC) analysis. PLA films used in this study were semicrystalline materials. They were characterized by the presence of glass transition, endothermic peak associated with it, and melting of crystals, clearly indicating the coexistence of amorphous and crystalline phases in the PLA physical structure (Figure 3).

The physical structure of semicrystalline polymers, such as PLA and other polyesters, is generally described by the three-phase model.[30,47,48] This model assumes that the semicrystalline physical structure cannot be explained as a simple coexistence of an undisturbed amorphous phase and a crystalline phase, without including a second and more rigid amorphous phase. The two amorphous regions are commonly named the "mobile amorphous phase" (MAP) and the "rigid amorphous fraction" (RAF). On the one hand, the MAP is the amorphous phase which behaves in a similar way than the fully amorphous polymer, having a similar glass transition temperature. On the other hand, the RAF is a fraction of the amorphous phase, which is closely associated with the crystalline phase. It is placed at the boundary between crystals and MAP. The mobility of the RAF polymer chains is highly restricted by the crystalline lamella, and it consequently behaves differently than MAP. RAF does not relax at the main glass transition temperature as MAP, but vitrificates at higher temperatures, between the MAP glass transition and melting of crystals, and depending on the polymer and processing sometimes at temperatures even higher than the melting temperature.[30,47−52] Although this transition is difficult to observe by conventional DSC analysis, its percentage in the polymer can easily be estimated from the measured variation of specific heat (ΔC_p) associated with the MAP glass transition and crystallinity percentage, as detailed in the Experimental Section.[30]

Thermograms (Figure 3) clearly showed that the amorphous phases and the crystalline phase of the PLA films were modified according to the time and to the storage conditions.

Modifications in the Mobile Amorphous Phase (MAP). *Endothermic Peak Associated with Glass Transition.* An endothermic peak associated with the glass transition was clearly noticeable in the PLA samples, as revealed by the first heating in DSC (Figure 3). Its area increased, and it was shifted to higher temperatures during time. A preliminary test indicated that these modifications occurred fast and were already displayed after only 2 days of storage. These thermal events were in agreement with the so-called physical aging of amorphous and semicrystalline polymers.[53,54] When a polymer is stored at temperatures lower than its T_g, slow molecular rearrangements occur, which densify the polymer structure. These rearrangements tend to decrease the excess of free energy and free volume of the polymer, and they are accelerated when the storage temperature is close to T_g. As a consequence, when the polymer is stored at $T < T_g$, it becomes more glass-like and less rubber-like during time, and an endothermic peak appears after the glass transition.[53,54]

An interesting effect of the water molecules in the shape of the endothermic peak associated with glass transition was also detected. It became progressively broader with increasing RH or when PLA is immersed in liquid water (Figure 3a). Such effect cannot be only attributed to the hydrolysis of PLA, since it was previously shown that during the first days of storage, the hydrolysis was very limited. In addition, no strong modification was observed in the endothermic peak shape—especially for samples stored at 85% RH—during the second month of storage (Figure 3b), when the impact of hydrolysis was undoubtful (Figure 2a,b). These findings thus indicated that water molecules played a key role in the physical interactions behind physical aging. Vyavahare et al.[55] has recently reported that water molecules increase the segmental mobility of PLA

DOI: 10.1021/acssuschemeng.6b03088
ACS Sustainable Chem. Eng. 2017, 5, 2751−2762

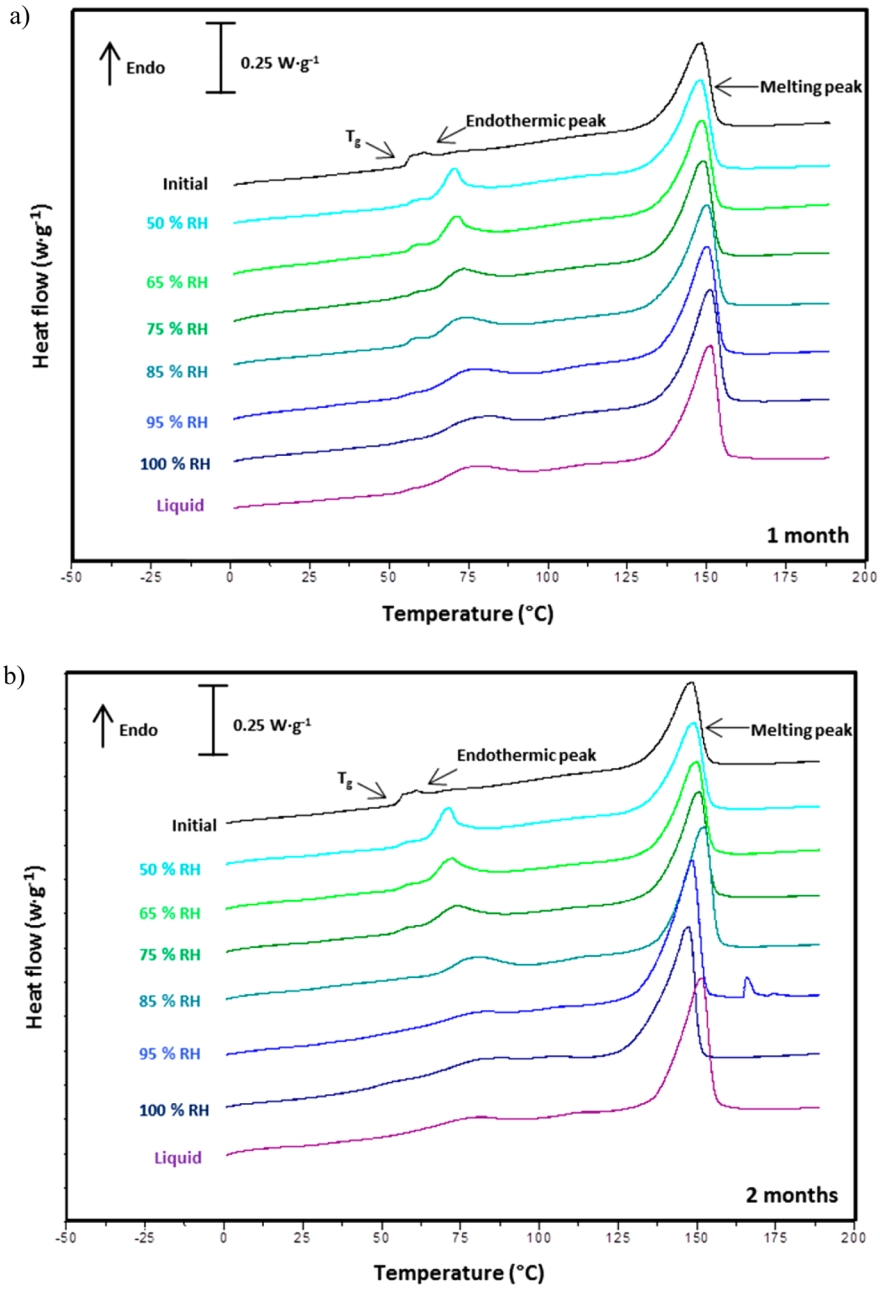

Figure 3. First heating DSC curves of PLA films from −10 to 190 °C to achieve complete melting. PLA films were aged at 50, 65, 75, 85, 95, or 100% RH or immersed in liquid water at 50 °C: (a) one month aging (28 days) and (b) two months aging (56 days).

chains and accelerate the kinetics of physical aging, as a consequence of the formation of water−water interactions (clusters) promoted by PLA carbonyl groups. Based on these considerations, it could be possible that the samples of the present study were characterized by increased water−water interactions at higher RH, which favored more heterogeneous molecular rearrangements.

Double-Step Glass Transition (T_{g1} and T_{g2}). The second heating in DSC, using lower temperatures program (from −10 to 100 °C), showed that the glass transition of MAP was actually constituted by a double step change, which was previously hindered by the endothermic peak related to physical aging, during the first heating (Figure 4). For the starting material, the inflection point of the first and second step was ∼55 and 65 °C, and the change in specific heat was ∼0.09 and 0.17 $J \cdot g^{-1} \cdot C^{-1}$, respectively. It is attributed to a consequence of the biorientation during processing. It is well known that this process modifies the PLA physical structure and promotes the formation of orientated PLA crystals within PLA amorphous chains.[56,57] Different studies have observed the existence of two (and close) glass transitions in semicrystalline PLA as a consequence of different crystallization processes.[31,58−60] According to the literature, these two different glass transitions confirm the presence of two amorphous mobile phases, one more mobile and the other more restricted. The more restricted phase is thought to be more associated with crystals, but differs from RAF since it is able to relax at temperatures higher, but rather close to that of the characteristic T_g of the material. Based on these considerations, both T_g steps were considered as individual transitions. The step at

DOI: 10.1021/acssuschemeng.6b03088
ACS Sustainable Chem. Eng. 2017, 5, 2751−2762

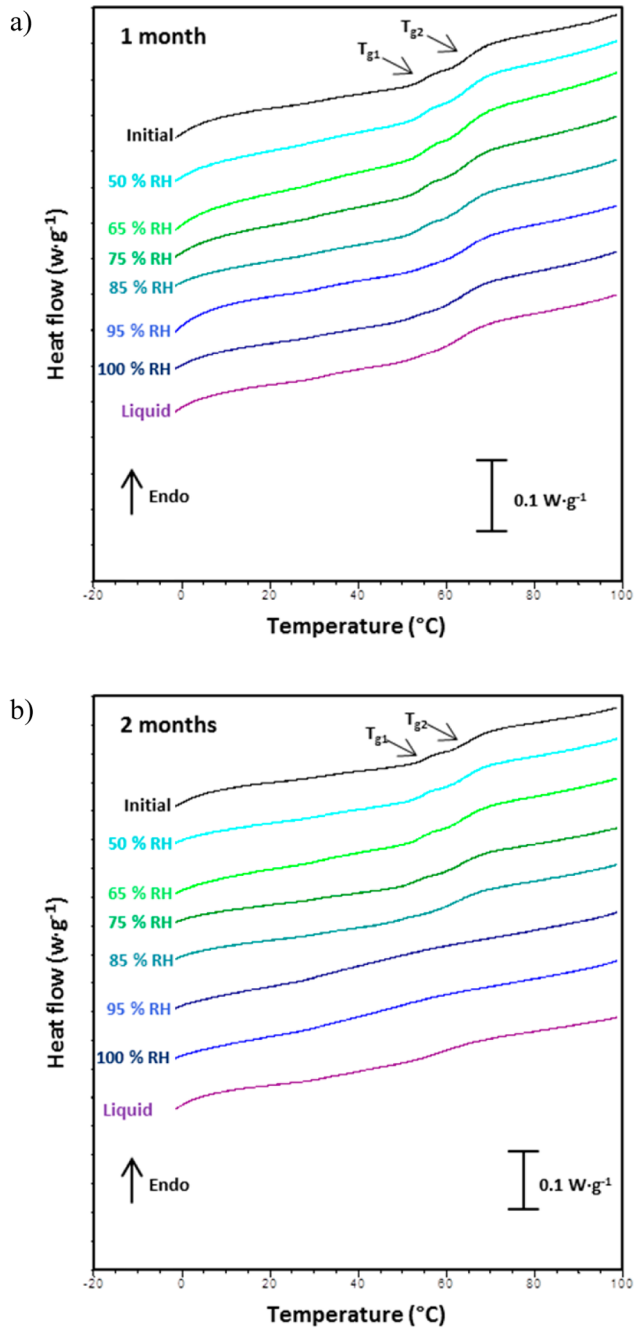

Figure 4. Second heating DSC curves of PLA films from −10 to 100 °C (final temperature stopped before melting). PLA films were aged at 50, 65, 75, 85, 95, or 100% RH or immersed in liquid water at 50 °C: (a) one month aging (28 days) and (b) two months aging (56 days).

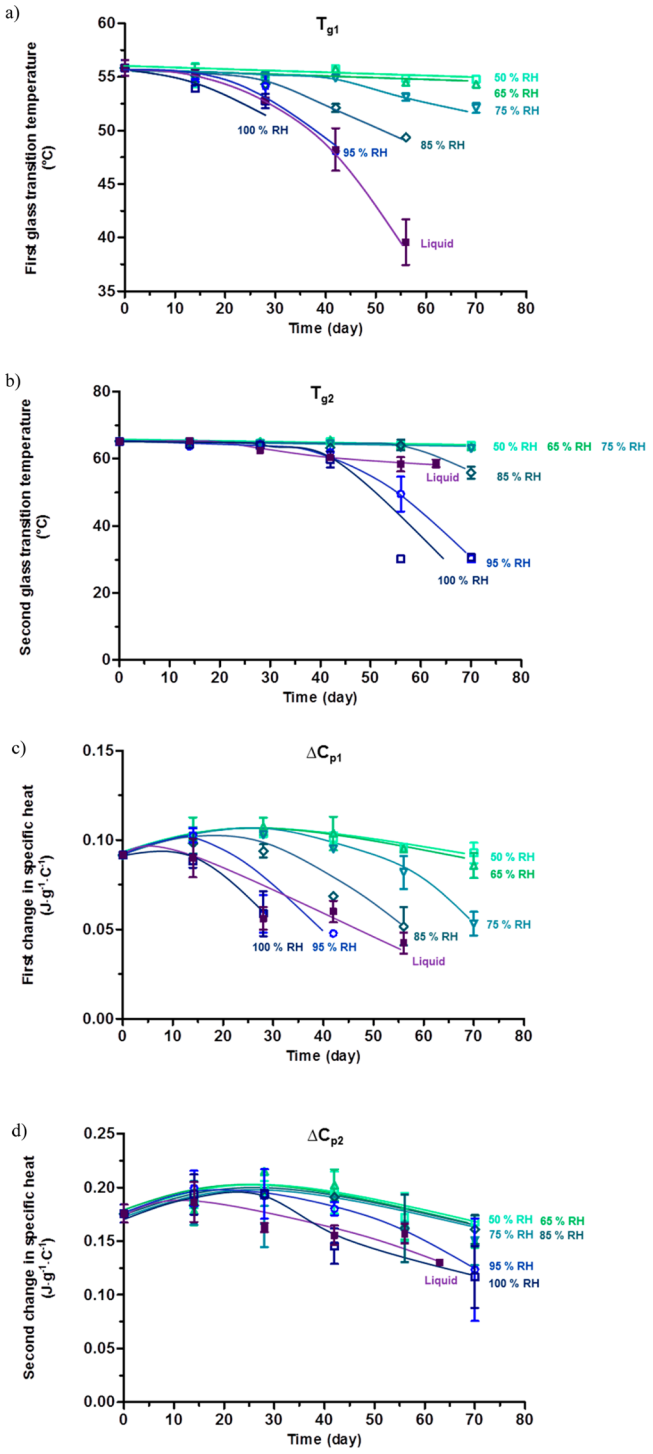

Figure 5. Modification in the thermal transitions related to mobile amorphous phase as a function of time for PLA films stored at 50, 65, 75, 85, 95, or 100% RH or immersed in liquid water at 50 °C: (a) first glass transition temperature (T_{g1}), (b) second glass transition temperature (T_{g2}), (c) first change in specific heat (ΔC_{p1}), and (d) second change in specific heat (ΔC_{p2}). Error bars are standard deviations. Lines are guides for the eyes.

lower temperature was referred to as T_{g1}, and the other one at higher temperature T_{g2}.

Figures 4 and 5a,b clearly show that T_{g1} and T_{g2} decreased during aging. The decrease trends were similar between them and are in accordance with the kinetics of hydrolysis (Figure 2a,b and Table 1): the decrease was as much pronounced as PLA was stored in environments at high RH or immersed in liquid water.

No strong modification was observed in the T_g of PLA samples stored at 50 and 65% RH, probably as a consequence of the reduced hydrolysis in such conditions, which apparently do not highly increase the mobility of PLA chains. On the contrary, the modifications were progressively stronger at RH > 65%, as expected from hydrolysis kinetics. Since the samples were dried before analyses, the decrease in both T_{g1} and T_{g2} cannot be attributed to a plasticizing effect of water, but to the

DOI: 10.1021/acssuschemeng.6b03088
ACS Sustainable Chem. Eng. 2017, 5, 2751−2762

lower molecular weight of PLA and to the plasticization effect of the small degradation products. Also in this case, the modifications of the PLA sample immersed in liquid water were slighter than for the samples stored at 100% RH, in agreement with the conclusions achieved from the previous section. Decreasing trends in T_g were also reported in other degradation studies of PLA involving water molecules in liquid and vapor phases.[25,26,36,44,61]

DSC analysis also indicated that both mobile amorphous phases had different water sensitivity, suggesting that the hydrolysis was faster in the mobile amorphous phase with the lower T_g. Such glass transition was no more detectable after 28, 42, 56, or 56 days when the PLA films were stored at 100, 95, or 85% RH or immersed in liquid water, respectively. On the contrary, the transition related to the more constrained MAP was always detectable (Figures 4 and 5a,b). The modifications of T_{g2} occurred mainly during the second month, while the modifications of T_{g1} were evidenced since the very first weeks of storage. In a similar way, ΔC_{p1} decreased much faster during the first month of storage than ΔC_{p2} (Figure 5cd). A possible explanation of this different water sensitivity in both MAP could be the different reduced mobility of the constrained MAP phase induced by crystals. It could be possible that the diffusion of water molecules is more difficult in that phase, reducing its reactivity.

Modifications in the Crystalline Phase. The crystalline phase of PLA was clearly modified during time, and in agreement with all of the analysis discussed, the modifications were progressively higher at increased RH (Figure 6).

The melting temperature (T_m) was constant (~149 °C) for the samples stored at 50% RH, but when the humidity increased, T_m slightly but significantly increased to ~151 °C. The samples stored at the conditions ≥85% RH were characterized by a further decrease in that value. After 70 days of storage the T_m of the samples stored at 85, 95, and 100% RH reached around 147, 135, and 133 °C, respectively. Similar increasing and then decreasing trend was also noticed by Tsuji and Ikada[26] and by Tsuji et al.[36] in PLA samples stored in phosphate buffer solutions at 37 °C for 3 years. According to these authors, the increase in T_m could be due to an increase in the thickness of PLA crystallites, which is promoted by the higher chain mobility induced by hydrolysis, favoring the thermostability of the crystals. On the contrary, the decrease of T_m indicates a reduction of the lamella thickness, which generates less thermostable crystals at increased aging times.

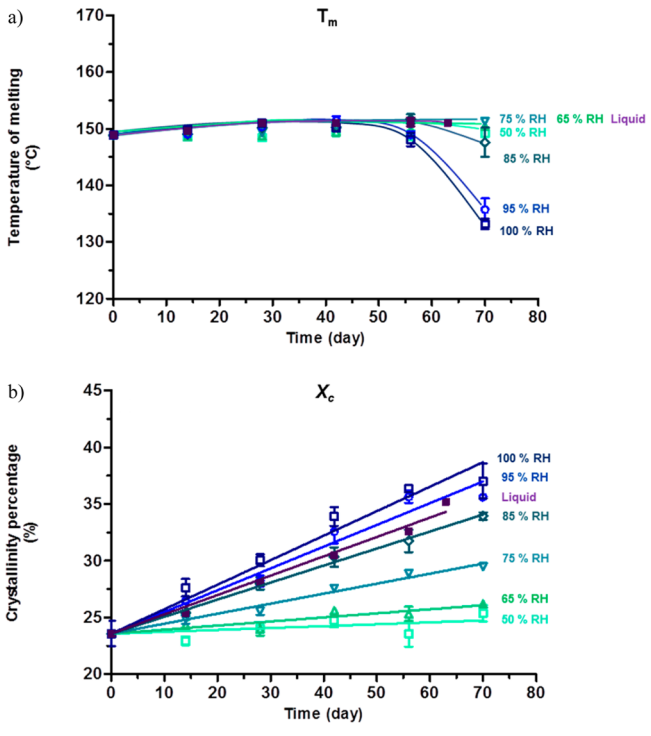

Figure 6. Modification in the thermal transitions related to the crystalline phase as a function of time for PLA films stored at 50, 65, 75, 85, 95, or 100% RH or immersed in liquid water at 50 °C: (a) melting temperature (T_m) and (b) crystallinity percentage (X_c). Error bars are standard deviations. Lines are guide for the eyes.

The crystallinity percentage (X_c) of PLA films was highly influenced by the storage conditions. When the samples were stored at 50% RH, no significant change in initial X_c (~23%) was observed, but when the RH increased or when the PLA samples were immersed in liquid water, the X_c linearly increased during time. As revealed by the kinetic analysis, such modifications followed an apparent zero order and had higher rates at increased RH (Table 1). X_c of the films kept at 65, 75, 85, 95, and 100% RH was ~26, 29, 34, 36, and 37% by the end of the storage test. When the PLA films were immersed in liquid water, X_c was between the values at 95 and 85% RH, confirming once again the deviation from the samples stored at 100% RH.

The increase of X_c is a well-known phenomenon in PLA under hydrolytic degradation, which occurs even in totally amorphous PLA. Hydrolysis-induced crystallization has been confirmed by different authors, using different techniques such as DSC, wide-angle X-ray scattering (WAXS), and Fourier transform infrared spectroscopy (FTIR). The increased chain mobility induced by the small degradation products and water molecules, which may favor plasticization and also crystallization of PLA chains.[22,24−26,33,41]

Modifications in the Rigid Amorphous Fraction (RAF). Initial PLA films contained a high quantity of rigid amorphous phase (X_{RAF} ~ 21%), which was around half quantity of the total mobile amorphous phase (X_{MAP} ~ 56%) and almost the same quantity of crystals (X_c ~ 23%). This indicated that the three-model phase was very well suited and would better describe the PLA physical structure than the two-phase model.

The changes in X_{RAF} and X_{MAP} during PLA aging are reported in Figure 7. From the trends of these graphs, it is worthy to note that both phases have almost an opposite behavior. When the hydrolysis is limited, X_{RAF} tends to decrease, while X_{MAP} tends to be constant or to slightly increase. When the hydrolysis is getting higher, X_{RAF} tends to increase, while X_{MAP} tends to decrease. A possible explanation of this behavior could be that when the hydrolysis is limited, part of the RAF becomes more mobile due to the plasticization induced by degradation products. When the hydrolysis is extended, part of MAP becomes more constrained due to the hydrolysis-induced crystallization of PLA, which most likely reduces the mobility of PLA chains and takes place more in MAP rather than in RAF.

These considerations can be considered in agreement with those of Tsuji and Miyauchi[62] from 2001, and Tsuji et al.[63] from 2005, who reported that the amorphous chains associated with RAF are much more hydrolysis-resistant in comparison to the amorphous chains related to MAP, from enzymatic

DOI: 10.1021/acssuschemeng.6b03088
ACS Sustainable Chem. Eng. 2017, 5, 2751−2762

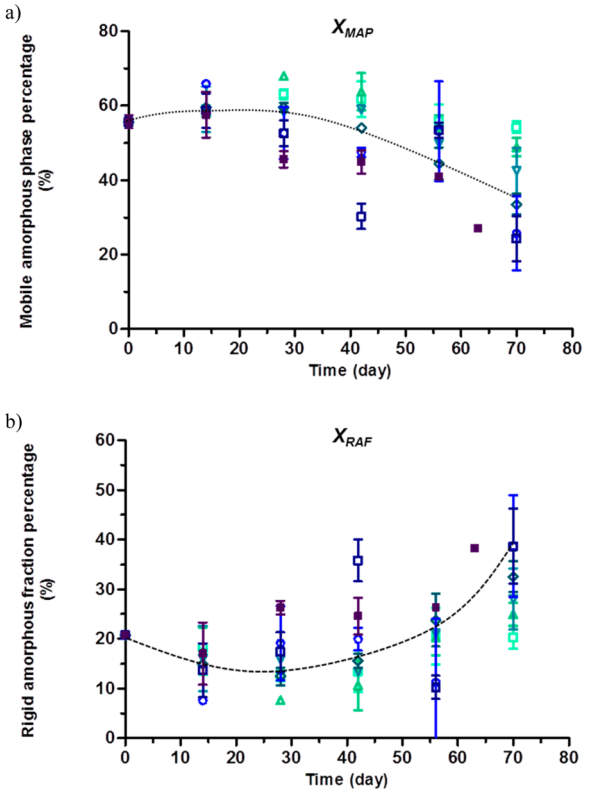

Figure 7. (a) Percentage of the mobile amorphous phase (X_{MAP}) and (b) percentage of the rigid amorphous fraction (X_{RAF}) of PLA films stored at 50, 65, 75, 85, 95, or 100% RH or immersed in liquid water at 50 °C as a function of time. Error bars are standard deviations. Lines are guides for the eyes.

degradation studies of PLA films conducted in alkaline environments (pH 8.6) at 37 °C.

CONCLUSION

This study gave a full depiction of the physical and chemical stability of PLA as thin films in a large range of RH environments and in contact with liquid water. Findings unambiguously showed that the PLA stability was influenced by the chemical potential and by the physical state of water molecules.

The macroscopic analyses pointed out an increased production of hydrophilic and acidic degradation products when the chemical potential of water increased. The behavior was different as a function of the physical state of water. When PLA was exposed to water vapor in a range from 50 to 100% RH, the degradation products were accumulated in the matrix, increasing water sorption and reactivity. When PLA was immersed in liquid water, the degradation products were solubilized and transferred to the aqueous medium, and no further water sorption occurred in the polymer.

The change in the molecular weight distribution ($\overline{M_n}$ and $\overline{M_w}$) confirmed that PLA was subjected to hydrolysis reaction for all of the storage conditions. The kinetic analysis revealed that the reaction was accelerated when the chemical potential of water increased. Nevertheless, the reaction was significantly slower when PLA was immersed in liquid water conditions compared to the 100% RH condition, even if water molecules had an equivalent chemical potential. Such deviation was a consequence of the accumulation of degradation products in PLA films at 100% RH, which also act as autocatalysts.

The physical structure of PLA suited very well with the three-model phase ($X_{RAF} + X_{MAP} + X_c = 100\%$). All the three phases were modified during hydrolysis. The rates of these modifications (T_{g1}, T_{g2}, ΔC_{p1}, ΔC_{p2}, T_m, X_c, X_{RAF}, X_{MAP}) matched in almost all the cases the trend from the kinetics of hydrolysis determined from SEC analysis: 50% RH < 65% RH < 75% RH < 85% RH < liquid <95% RH < 100% RH. When the hydrolysis was favored X_{RAF} increased, X_{MAP} decreased, and X_c increased. Thus, this indicated that hydrolysis induced crystallization of MAP polymer chains, which in turn constrained additional MAP chains, transforming them into RAF.

From a practical point of view, the findings of this research can be used as strong scientific basis for giving recommendations about the use of this material and for estimating its shelf life in its applications as packaging or mulch films.

AUTHOR INFORMATION

Corresponding Author

*Tel.: +33 380 77 2388. Fax: +33 380 77 40 11. E-mail: thomas.karbowiak@u-bourgogne.fr.

ORCID

Thomas Karbowiak: 0000-0002-4229-3003

Notes

The authors declare no competing financial interest.

ACKNOWLEDGMENTS

The authors acknowledge the European Social Fund - Friuli Venezia Giulia Region - Operational Program 2007/2013 for supporting this project (Regional code: FP1340303009), the Università Italo-Francese for mobility grant (Bando Vinci 2015 Cap II, project code C2-64), the RMB plateau of UMR PAM for thermal analyses, and the ICMUB research unit for SEC analyses.

REFERENCES

(1) Halden, R. U. Plastics and health risks. *Annu. Rev. Public Health* **2010**, *31*, 179−194.

(2) Thompson, R. C.; Moore, C. J.; vom Saal, F. S.; Swan, S. H. Plastics, the environment and human health: current consensus and future trends. *Philos. Trans. R. Soc., B* **2009**, *364* (1526), 2153−2166.

(3) Teuten, E. L.; Saquing, J. M.; Knappe, D. R. U.; Barlaz, M. A.; Jonsson, S.; Bjorn, A.; Rowland, S. J.; Thompson, R. C.; Galloway, T. S.; Yamashita, R.; Ochi, D.; Watanuki, Y.; Moore, C.; Viet, P. H.; Tana, T. S.; Prudente, M.; Boonyatumanond, R.; Zakaria, M. P.; Akkhavong, K.; Ogata, Y.; Hirai, H.; Iwasa, S.; Mizukawa, K.; Hagino, Y.; Imamura, A.; Saha, M.; Takada, H. Transport and release of chemicals from plastics to the environment and to wildlife. *Philos. Trans. R. Soc., B* **2009**, *364* (1526), 2027−2045.

(4) European Bioplastics Association. Global production capacities of bioplastics 2014 (by material type) and applications (2016), http://en.european-bioplastics.org/market (accessed Dec 9, 2016).

(5) Reddy, M. M.; Vivekanandhan, S.; Misra, M.; Bhatia, S. K.; Mohanty, A. K. Biobased plastics and bionanocomposites: current status and future opportunities. *Prog. Polym. Sci.* **2013**, *38* (10−11), 1653−1689.

(6) Mekonnen, T.; Mussone, P.; Khalil, H.; Bressler, D. Progress in bio-based plastics and plasticizing modifications. *J. Mater. Chem. A* **2013**, *1* (43), 13379−13398.

(7) Castro-Aguirre, E.; Iñiguez-Franco, F.; Samsudin, H.; Fang, X.; Auras, R. Poly(lactic acid)—Mass production, processing, industrial

DOI: 10.1021/acssuschemeng.6b03088
ACS Sustainable Chem. Eng. 2017, 5, 2751−2762

applications, and end of life. *Adv. Drug Delivery Rev.* **2016**, *107*, 333−366.
(8) Auras, R.; Harte, B.; Selke, S. An overview of polylactides as packaging materials. *Macromol. Biosci.* **2004**, *4* (9), 835−864.
(9) Jamshidian, M.; Tehrany, E. A.; Imran, M.; Jacquot, M.; Desobry, S. Poly-lactic acid: production, applications, nanocomposites, and release studies. *Compr. Rev. Food Sci. Food Saf.* **2010**, *9* (5), 552−571.
(10) Tan, B. H.; Muiruri, J. K.; Li, Z.; He, C. Recent progress in using stereocomplexation for enhancement of thermal and mechanical property of polylactide. *ACS Sustainable Chem. Eng.* **2016**, *4* (10), 5370−5391.
(11) Corneillie, S.; Smet, M. PLA architectures: the role of branching. *Polym. Chem.* **2015**, *6* (6), 850−867.
(12) Kai, D.; Ren, W.; Tian, L.; Chee, P. L.; Liu, Y.; Ramakrishna, S.; Loh, X. J. Engineering poly(lactide)−lignin nanofibers with antioxidant activity for biomedical application. *ACS Sustainable Chem. Eng.* **2016**, *4* (10), 5268−5276.
(13) Agustin-Salazar, S.; Gamez-Meza, N.; Medina-Juàrez, L. À.; Soto-Valdez, H.; Cerruti, P. From nutraceutics to materials: effect of resveratrol on the stability of polylactide. *ACS Sustainable Chem. Eng.* **2014**, *2* (6), 1534−1542.
(14) Armentano, I.; Bitinis, N.; Fortunati, E.; Mattioli, S.; Rescignano, N.; Verdejo, R.; Lopez-Manchado, M. A.; Kenny, J. M. Multifunctional nanostructured PLA materials for packaging and tissue engineering. *Prog. Polym. Sci.* **2013**, *38* (10−11), 1720−1747.
(15) Zhu, H. G.; Ji, J.; Shen, J. C. Surface engineering of poly(DL-lactic acid) by entrapment of biomacromolecules. *Macromol. Rapid Commun.* **2002**, *23* (14), 819−823.
(16) Fabra, M. J.; Busolo, M. A.; Lopez-Rubio, A.; Lagaron, J. M. Nanostructured biolayers in food packaging. *Trends Food Sci. Technol.* **2013**, *31* (1), 79−87.
(17) Rocca-Smith, J. R.; Karbowiak, T.; Marcuzzo, E.; Sensidoni, A.; Piasente, F.; Champion, D.; Heinz, O.; Vitry, P.; Bourillot, E.; Lesniewska, E.; Debeaufort, F. Impact of corona treatment on PLA film properties. *Polym. Degrad. Stab.* **2016**, *132*, 109−116.
(18) Janorkar, A. V.; Metters, A. T.; Hirt, D. E. Modification of poly(lactic acid) films: enhanced wettability from surface-confined photografting and increased degradation rate due to an artifact of the photografting process. *Macromolecules* **2004**, *37* (24), 9151−9159.
(19) Rasal, R. M.; Janorkar, A. V.; Hirt, D. E. Poly(lactic acid) modifications. *Prog. Polym. Sci.* **2010**, *35* (3), 338−356.
(20) Wang, S. G.; Cui, W. J.; Bei, J. Z. Bulk and surface modifications of polylactide. *Anal. Bioanal. Chem.* **2005**, *381* (3), 547−556.
(21) Witzke, D. R. Introduction to properties, engineering, and prospects of polylactide polymers. PhD. Dissertation, Michigan State University, East Lansing, MI, 1997.
(22) Gorrasi, G.; Pantani, R. Effect of PLA grades and morphologies on hydrolytic degradation at composting temperature: Assessment of structural modification and kinetic parameters. *Polym. Degrad. Stab.* **2013**, *98* (5), 1006−1014.
(23) Li, S. M. Hydrolytic degradation characteristics of aliphatic polyesters derived from lactic and glycolic acids. *J. Biomed. Mater. Res.* **1999**, *48* (3), 342−353.
(24) Tsuji, H. Hydrolytic degradation. In *Poly(lactic acid): synthesis, structures, properties, processing, and applications*; Auras, R., Lim, L.-T., Selke, S. E. M., Tsuji, H., Eds.; Wiley: Hoboken, NJ, 2010.
(25) Migliaresi, C.; Fambri, L.; Cohn, D. A study on the in-vitro degradation of poly(lactic acid). *J. Biomater. Sci., Polym. Ed.* **1994**, *5* (6), 591−606.
(26) Tsuji, H.; Ikada, Y. Properties and morphology of poly(L-lactide) 4. Effects of structural parameters on long-term hydrolysis of poly(L-lactide) in phosphate-buffered solution. *Polym. Degrad. Stab.* **2000**, *67* (1), 179−189.
(27) Makino, K.; Arakawa, M.; Kondo, T. Preparation and invitro degradation properties of polylactide microcapsules. *Chem. Pharm. Bull.* **1985**, *33* (3), 1195−1201.
(28) Greenspan, L. Humidity fixed points of binary saturated aqueous solutions. *J. Res. Natl. Bur. Stand., Sect. A* **1977**, *81* (1), 89−96.
(29) Fischer, E. W.; Sterzel, H. J.; Wegner, G. Investigation of the structure of solution grown crystals of lactide copolymers by means of chemical reactions. *Kolloid Z. Z. Polym.* **1973**, *251*, 980−990.
(30) Arnoult, M.; Dargent, E.; Mano, J. F. Mobile amorphous phase fragility in semi-crystalline polymers: Comparison of PET and PLLA. *Polymer* **2007**, *48* (4), 1012−1019.
(31) Delpouve, N.; Arnoult, M.; Saiter, A.; Dargent, E.; Saiter, J. M. Evidence of two mobile amorphous phases in semicrystalline polylactide observed from calorimetric investigations. *Polym. Eng. Sci.* **2014**, *54* (5), 1144−1150.
(32) Holm, V. K.; Ndoni, S.; Risbo, J. The stability of poly(lactic acid) packaging films as influenced by humidity and temperature. *J. Food Sci.* **2006**, *71* (2), E40−E44.
(33) Kucharczyk, P.; Hnatkova, E.; ZdenekDvorak; Sedlarik, V. Novel aspects of the degradation process of PLA based bulky samples under conditions of high partial pressure of water vapour. *Polym. Degrad. Stab.* **2013**, *98* (1), 150−157.
(34) Cairncross, R. A.; Becker, J. G.; Ramaswamy, S.; O'Connor, R. Moisture sorption, transport, and hydrolytic degradation in polylactide. *Appl. Biochem. Biotechnol.* **2006**, *131* (1−3), 774−785.
(35) Lyu, S. P.; Schley, J.; Loy, B.; Lind, D.; Hobot, C.; Sparer, R.; Untereker, D. Kinetics and time-temperature equivalence of polymer degradation. *Biomacromolecules* **2007**, *8* (7), 2301−2310.
(36) Tsuji, H.; Mizuno, A.; Ikada, Y. Properties and morphology of poly(L-lactide). III. Effects of initial crystallinity on long-term in vitro hydrolysis of high molecular weight poly(L-lactide) film in phosphate-buffered solution. *J. Appl. Polym. Sci.* **2000**, *77* (7), 1452−1464.
(37) Tsuji, H. Poly(lactide) stereocomplexes: Formation, structure, properties, degradation, and applications. *Macromol. Biosci.* **2005**, *5* (7), 569−597.
(38) Li, S. M.; McCarthy, S. Further investigations on the hydrolytic degradation of poly(DL-lactide). *Biomaterials* **1999**, *20* (1), 35−44.
(39) Mitchell, M. K.; Hirt, D. E. Degradation of PLA fibers at elevated temperature and humidity. *Polym. Eng. Sci.* **2015**, *55* (7), 1652−1660.
(40) Olewnik-Kruszkowska, E. Influence of the type of buffer solution on thermal and structural properties of polylactide-based composites. *Polym. Degrad. Stab.* **2016**, *129*, 87−95.
(41) Harris, A. M.; Lee, E. C. Heat and humidity performance of injection molded PLA for durable applications. *J. Appl. Polym. Sci.* **2010**, *115* (3), 1380−1389.
(42) Ho, K. L. G.; Pometto, A. L., III; Hinz, P. N. Effects of temperature and relative humidity on polylactic acid plastic degradation. *J. Polym. Environ.* **1999**, *7* (2), 83−92.
(43) Mohd-Adnan, A.-F.; Nishida, H.; Shirai, Y. Evaluation of kinetics parameters for poly(l-lactic acid) hydrolysis under high-pressure steam. *Polym. Degrad. Stab.* **2008**, *93* (6), 1053−1058.
(44) Copinet, A.; Bertrand, C.; Govindin, S.; Coma, V.; Couturier, Y. Effects of ultraviolet light (315 nm), temperature and relative humidity on the degradation of polylactic acid plastic films. *Chemosphere* **2004**, *55* (5), 763−773.
(45) Hakkarainen, M.; Karlsson, S.; Albertsson, A. C. Rapid (bio)degradation of polylactide by mixed culture of compost microorganisms - low molecular weight products and matrix changes. *Polymer* **2000**, *41* (7), 2331−2338.
(46) Gleadall, A.; Pan, J.; Kruft, M.-A.; Kellomaki, M. Degradation mechanisms of bioresorbable polyesters. Part 1. Effects of random scission, end scission and autocatalysis. *Acta Biomater.* **2014**, *10* (5), 2223−2232.
(47) Wunderlich, B. Reversible crystallization and the rigid−amorphous phase in semicrystalline macromolecules. *Prog. Polym. Sci.* **2003**, *28* (3), 383−450.
(48) Kattan, M.; Dargent, E.; Grenet, J. Three phase model in drawn thermoplastic polyesters: comparison of differential scanning calorimetry and thermally stimulated depolarisation current experiments. *Polymer* **2002**, *43* (4), 1399−1405.
(49) Magoń, A.; Pyda, M. Study of crystalline and amorphous phases of biodegradable poly(lactic acid) by advanced thermal analysis. *Polymer* **2009**, *50* (16), 3967−3973.

DOI: 10.1021/acssuschemeng.6b03088
ACS Sustainable Chem. Eng. 2017, 5, 2751−2762

(50) Bai, H.; Huang, C.; Xiu, H.; Zhang, Q.; Fu, Q. Enhancing mechanical performance of polylactide by tailoring crystal morphology and lamellae orientation with the aid of nucleating agent. *Polymer* **2014**, *55* (26), 6924−6934.
(51) Delpouve, N.; Delbreilh, L.; Stoclet, G.; Saiter, A.; Dargent, E. Structural dependence of the molecular mobility in the amorphous fractions of polylactide. *Macromolecules* **2014**, *47* (15), 5186−5197.
(52) Righetti, M. C.; Tombari, E. Crystalline, mobile amorphous and rigid amorphous fractions in poly(L-lactic acid) by TMDSC. *Thermochim. Acta* **2011**, *522* (1−2), 118−127.
(53) Hutchinson, J. M. Physical aging of polymers. *Prog. Polym. Sci.* **1995**, *20* (4), 703−760.
(54) Struik, L. C. E. Physical aging in plastics and other glassy materials. *Polym. Eng. Sci.* **1977**, *17* (3), 165−173.
(55) Vyavahare, O.; Ng, D.; Hsu, S. L. Analysis of structural rearrangements of poly(lactic acid) in the presence of water. *J. Phys. Chem. B* **2014**, *118* (15), 4185−4193.
(56) Delpouve, N.; Stoclet, G.; Saiter, A.; Dargent, E.; Marais, S. Water barrier properties in biaxially drawn poly(lactic acid) films. *J. Phys. Chem. B* **2012**, *116* (15), 4615−4625.
(57) Jariyasakoolroj, P.; Tashiro, K.; Wang, H.; Yamamoto, H.; Chinsirikul, W.; Kerddonfag, N.; Chirachanchai, S. Isotropically small crystalline lamellae induced by high biaxial-stretching rate as a key microstructure for super-tough polylactide film. *Polymer* **2015**, *68*, 234−245.
(58) Righetti, M. C.; Prevosto, D.; Tombari, E. Time and temperature evolution of the rigid amorphous fraction and differently constrained amorphous fractions in PLLA. *Macromol. Chem. Phys.* **2016**, *217* (18), 2013−2026.
(59) Dionisio, M.; Viciosa, M. T.; Wang, Y. M.; Mano, J. F. Glass transition dynamics of poly(L-lactic acid) during isothermal crystallisation monitored by real-time dielectric relaxation spectroscopy measurements. *Macromol. Rapid Commun.* **2005**, *26* (17), 1423−1427.
(60) Wang, Y.; Ribelles, J. L. G.; Sanchez, M. S.; Mano, J. F. Morphological contributions to glass transition in poly(L-lactic acid). *Macromolecules* **2005**, *38* (11), 4712−4718.
(61) Gonzalez, M. F.; Ruseckaite, R. A.; Cuadrado, T. R. Structural changes of polylactic-acid (PLA) microspheres under hydrolytic degradation. *J. Appl. Polym. Sci.* **1999**, *71* (8), 1223−1230.
(62) Tsuji, H.; Miyauchi, S. Poly(l-lactide): 7. Enzymatic hydrolysis of free and restricted amorphous regions in poly(l-lactide) films with different crystallinities and a fixed crystalline thickness. *Polymer* **2001**, *42* (9), 4463−4467.
(63) Tsuji, H.; Tezuka, Y.; Yamada, K. Alkaline and enzymatic degradation of L-lactide copolymers. II. Crystallized films of poly(L-lactide-co-D-lactide) and poly(L-lactide) with similar crystallinities. *J. Polym. Sci., Part B: Polym. Phys.* **2005**, *43* (9), 1064−1075.

DOI: 10.1021/acssuschemeng.6b03088
ACS Sustainable Chem. Eng. 2017, 5, 2751−2762